

# Anti-4-1BB antibody-based combination therapy augments antitumor immunity by enhancing CD11c<sup>+</sup>CD8<sup>+</sup> T cells in renal cell carcinoma

SEONG-A JU<sup>1</sup>, SANG-MIN PARK<sup>2</sup>, YEONSOO JOE<sup>1</sup>, HUN TAEG CHUNG<sup>1</sup>, WON G. AN<sup>3</sup> and BYUNG-SAM KIM<sup>1</sup>

<sup>1</sup>School of Biological Sciences, University of Ulsan, Ulsan 44610;

<sup>2</sup>CEFO Co., Ltd., Seoul 03150; <sup>3</sup>Division of Pharmacology, School of Korean Medicine, Pusan National University, Yangsan, Gyeongsangnam 50612, Republic of Korea

Received August 10, 2021; Accepted November 12, 2021

DOI: 10.3892/ol.2021.13161

**Abstract.** To improve the potential treatment strategies of incurable renal cell carcinoma (RCC), which is highly resistant to chemotherapy and radiotherapy, the present study established a combination therapy with immunostimulatory factor (ISTF) and anti-4-1BB monoclonal antibodies (mAbs) to augment the antitumor response in a murine RCC model. ISTF isolated from *Actinobacillus actinomycetemcomitans* stimulates macrophages, dendritic cells and B cells to produce IL-6, TNF- $\alpha$ , nitric oxide and major histocompatibility complex class II expression. 4-1BB (CD137) is expressed in activated immune cells, including activated T cells, and is a promising target for cancer immunotherapy. The administration of anti-4-1BB mAbs promoted antitumor immunity via enhancing CD11c<sup>+</sup>CD8<sup>+</sup> T cells. The CD11c<sup>+</sup>CD8<sup>+</sup> T cells were characterized by high killing activity and IFN- $\gamma$ -producing ability, representing a phenotype of active effector cytotoxic T lymphocytes. The present study showed that combination therapy with ISTF and anti-4-1BB mAbs promoted partial tumor regression with established RCC, but monotherapy with ISTF or anti-4-1BB mAbs did not. These effects were speculated to be caused by the increase in CD11c<sup>+</sup>CD8<sup>+</sup> T cells in the spleen and tumor, and IFN- $\gamma$  production. These insights into the effector mechanisms of the combination of ISTF and anti-4-1BB mAbs may be useful for targeting incurable RCC.

## Introduction

Renal cell carcinoma (RCC) is the most common form of kidney cancer. Its incidence has steadily risen over the past 10 years, and it accounts for 2-3% of all adult malignancies (1). RCC cells show high multidrug resistance, which makes chemotherapy ineffective, and radiotherapy can only relieve the symptoms (2). RCC cells have a lower rate of cleavage than other cancer cells, which is speculated to be a cause of resistance to chemotherapy and radiotherapy (3,4). Due to the poor response of RCC to radiotherapy and chemotherapy, the 5-year survival rate for metastatic RCC is only 10% (5). Previously, treatment of RCC was rare and was occasionally managed by the patient's own immune system (2). For this reason, immunotherapy using IFN- $\gamma$  and IL-2 has been experimentally used for the treatment of RCC (6-8). However, several clinical applications of IFN- $\gamma$  and IL-2 immunotherapy have shown that the overall prognosis of patients remains poor, with only 20% of patients responding for short periods of time; the therapy also induces severe toxicity (9). Due to these disappointing outcomes, the development of novel therapies for RCC is urgent, and a number of studies are now being conducted worldwide.

4-1BB (CD137) is expressed on activated T cells and delivers co-stimulatory signals for T cell activation when it binds to 4-1BB ligand or in ligation with agonistic anti-4-1BB monoclonal antibodies (mAbs) (10,11). The systemic administration of agonistic anti-4-1BB mAbs to tumor-bearing mice with P815 mastocytoma, AG104A sarcoma (12), B10.2 fibrosarcoma (13) and CT26 colon carcinoma (14) caused tumor regression, but they had no effect on weakly or poorly immunogenic tumors, such as B16 melanoma, C3 tumors and TC-1 lung carcinoma (15). Researchers have tested the efficacy of combinations of anti-4-1BB mAbs and various reagents to enhance the anticancer effects. Previously, using a murine RCC tumor model, we showed that a combination of subtoxic doses of fluorouracil (5-FU) and anti-4-1BB mAb eradicated established tumors, while either 5-FU or anti-4-1BB mAb monotherapy did not (16). In addition, immune checkpoint blockade in combination with anti-VEGF or anti-programmed cell death protein 1 (PD-1) have been

**Correspondence to:** Professor Won G. An, Division of Pharmacology, School of Korean Medicine, Pusan National University, 49 Pusan Daehak-ro, Yangsan, Gyeongsangnam 50612, Republic of Korea  
E-mail: wgan@pusan.ac.kr

Professor Byung-Sam Kim, School of Biological Sciences, University of Ulsan, 93 Deahak-ro, Nam-gu, Ulsan 44610, Republic of Korea  
E-mail: bskim@ulsan.ac.kr

**Key words:** renal cell carcinoma, 4-1BB, immunostimulating factor, CD11c<sup>+</sup>CD8<sup>+</sup> T cells, IFN- $\gamma$

found to augment T cell-mediated antitumor immunity in metastatic RCC (17,18). The expression of PD-1 on 4-1BB T cells may be novel therapeutic targets for immunotherapy of metastatic RCC (19,20).

*Actinobacillus actinomycetemcomitans* (*A. actinomycetemcomitans*) is associated with several human diseases, including endocarditis, meningitis, osteomyelitis, subcutaneous abscesses and periodontal disease (21-25). The immunostimulatory factor (ISTF; 13 kDa) isolated from *A. actinomycetemcomitans*, has potent mitogenic activity on mouse B cells and human peripheral blood mononuclear cells (26). ISTF has been reported to stimulate macrophages and dendritic cells in the spleens of BALB/c mice and also has the ability to induce the direct activation of mouse macrophages to induce IL-6, TNF- $\alpha$ , nitric oxide and major histocompatibility complex (MHC) class II expression (27). In addition, ISTF is a proteinaceous material that directly induces the proliferation of B lymphocytes, but does not affect the proliferation of T lymphocytes, even in the presence of antigen-presenting cells (APCs) (26).

To fully activate T cells, both antigen recognition (peptide and MHC complex) and co-stimulatory signals provided by APCs are required (28). In the absence of co-stimulatory signals, antigen presentation induces T cell anergy, while co-stimulatory signals activate non-responding tumor-specific T cells (29). ISTF is expected to be highly active against APCs, and anticancer activity can be expected to be increased by the amplification of the overall immune response (27). Therefore, in the present study it was hypothesized that a combination of ISTF, promoting antigen presentation, and 4-1BB mAbs, stimulating T cell co-stimulation signals, could increase T cell activity to eradicate RCC. The aim of this study was to evaluate the efficacy of a combination of ISTF and agonistic anti-4-1BB mAbs in the RCC model, which is associated with multidrug resistance and does not respond well to anticancer therapy.

## Materials and methods

**Animals and reagents.** Female Balb/c mice (7 weeks of age, 156 mice) were purchased from Orient Bio, Inc. The mice were housed under specific pathogen-free conditions at 18-24°C and 40-70% humidity in a 12 h light-dark cycle, with *ad libitum* access to food and water. Animal studies were approved by the University of Ulsan Animal Care and Use Committee (approval no. HTC-14-030; Nam-gu, Republic of Korea). All mice were subjected to anesthesia by tribromoethanol [intraperitoneally (i.p.) injection, 250 mg/kg, 30 min] or euthanasia by using a flow rate of 3-7 liters per min with CO<sub>2</sub> for a 10-liter volume. Hybridomas (Clone 3E1) producing agonistic anti-4-1BB mAb were a gift from Dr Robert Mittler (Emory University, Atlanta, GA, USA). Anti-CD3 monoclonal antibody (cat. no. 557306), FITC-CD3 (cat. no. 553061), PE-CD8 (cat. no. 553032), FITC-CD8 (cat. no. 553030), PerCP-Cy<sup>TM</sup> 5.5-CD8 (cat. no. 551162), PE-B220 (cat. no. 553089), PerCP-Cy<sup>TM</sup> 5.5-CD4 (cat. no. 550954), PE-CD4 (cat. no. 557308), PE-Foxp3 (cat. no. 560408), PE-F4/80 (cat. no. 565410), PE-DX5 (cat. no. 553858), PE-CD11b (cat. no. 557397), FITC-Gr1 (cat. no. 553126), PE-CD11c (cat. no. 557401), FITC-CD11c

(cat. no. 557400), PE-IFN- $\gamma$  (cat. no. 562020) were purchased from BD Pharmingen (BD Biosciences). The gene encoding an ISTF from *Actinobacillus actinomycetemcomitans* was cloned into the pET-32a(+) DNA-Novagen expression vector (Sigma-Aldrich; Merck KGaA). The recombinant vector containing a full-length ISTF gene fused with a C-terminal His6 tag was transformed into *E. coli* BL21 (DE3; Stratagene; Agilent Technologies, Inc.). The expression of the recombinant ISTF was induced by incubation with 1 mM isopropyl  $\beta$ -D-1-thiogalactopyranoside (IPTG; Sigma-Aldrich; Merck KGaA) at 20°C for 4 h, and the recombinant ISTF was purified using a Protino<sup>®</sup> Ni-TED column (Machery-Nagel GmbH) according to the manufacturer's protocols.

**Tumor cells and animal experiments.** Renca cells were purchased from the Korean Cell Line Bank (Korean Cell Line Research Foundation) and cultured in RPMI-1640 medium (Gibco; Thermo Fisher Scientific, Inc.) supplemented with 10% FBS (Gibco; Thermo Fisher Scientific, Inc.). For the animal experiments, log-phase cells were washed and resuspended in PBS immediately before injection into mice. Mice weighing 20 $\pm$ 0.5 g were subcutaneously (s.c.) injected with Renca tumor cells into the site over the right flank (1 $\times$ 10<sup>6</sup>/mouse, 100  $\mu$ l). ISTF was injected i.p. on days 3, 7 and 12, and anti-4-1BB mAb (3E1) was injected i.p. on days 7 and 12, while a control group received PBS and rat IgG (16,27). The tumor diameter was measured every 2-3 days, and the tumor volume (in mm<sup>3</sup>) was calculated using a caliper. The tumor size was expressed as the tumor volume based on the following formula: Tumor volume (mm<sup>3</sup>)  $\times$  (major axis)  $\times$  (minor axis)  $\times$  (height)  $\times$  0.52. The animals were sacrificed when the longest dimensions of the tumors were >20 mm. Mice were considered tumor free when the tumor dimensions were <1 mm; they were kept under observation for at least 60 days. At least 6-10 mice/treatment group were examined throughout the day, and each reported experiment was representative of at least three similarly performed experiments.

**Isolation of splenocytes.** The murine spleen was placed in a petri dish with 5 ml Hanks' balanced salt solution buffer, and the spleen was cut into small pieces ( $\sim$ 0.2 cm<sup>2</sup>) with a scalpel blade. The small pieces were crushed using the plunger end of a syringe and then the cell suspensions were passed through a cell strainer. After centrifugation (220  $\times$  g, 5 min, 4°C) the cell pellet was suspended in 2-5 ml cold 1X RBC Lysis buffer (eBioscience; Thermo Fisher Scientific, Inc.). After incubating the suspension for 5 min on ice, cells were washed with 10-20 ml cold PBS. Cells (1 $\times$ 10<sup>6</sup> cells/ml) were suspended in 1% BSA (Roche Diagnostics) in PBS for fluorescence activated cell sorting (FACS) analysis or in RPMI-1640 medium for cytokine analysis.

**Isolation of tumor-infiltrating lymphocytes (TILs) from tumor tissue.** TILs were isolated from tumor tissues as described previously (30) with minor modifications. Briefly, tumors were excised (2-3 mm in width), and the fragments were incubated in RPMI-1640 medium containing 10% FBS, collagenase type I (300 U/ml; Gibco; Thermo Fisher Scientific, Inc.) and DNase I (50 U/ml; Sigma-Aldrich; Merck KGaA) at 37°C for 90 min. Thereafter, the digested fragments were passed through steel mesh, layered over superimposed layers of 54 and 63% Percoll

and centrifuged at 400 x g for 45 min at room temperature. TILs were recovered at the interface between 54 and 63% of the Percoll layers.

**Surgical removal of tumor-draining lymph nodes (TDLNs).** At day 14 after injection with ISTF and anti-4-BB mAb, tumor-bearing mice were subjected to surgical removal of the adjacent inguinal lymph nodes (3).

**Hepatocellular damage assay.** To detect serum alanine aminotransferase (ALT) and aspartate aminotransferase (AST), serum was collected by centrifugation at 585 x g for 15 min at 4°C from peripheral blood obtained through the retro-orbital bleeding procedure. ALT and AST activity, indicators of hepatocellular injury, were measured using the Enzy-Chrom™ Alanine Transaminase Assay Kit (cat. no. EALT-100; BioAssay Systems) and Enzy-Chrom™ Aspartate Transaminase Assay Kit (cat. no. EASTR-100; BioAssay Systems).

**FACS analysis.** For FACS analysis, splenocytes and TILs were blocked with the Fc receptor-blocking mAb 2.4G2 for 20 min at 4°C and stained with 4G2, FITC-CD3, PE-CD4, PE-CD8, PE-DX5, PE-CD11b and FITC-CD11c mAbs for 30 min at 4°C. After washing, they were analyzed with a FACSCalibur flow cytometer (Becton, Dickinson and Company). Data were analyzed by using FlowJo v10 software (FlowJo LLC).

**Determination of intracellular cytokines.** To measure the expression of IFN- $\gamma$ , spleens were isolated from Renca-bearing mice on day 14 and cultured with PMA (50 ng/ml; Sigma-Aldrich; Merck KGaA) and ionomycin (500 ng/ml; Sigma-Aldrich; Merck KGaA), and cytokine release was prevented by treatment with Golgi-stop (BD Pharmingen; BD Biosciences). Following surface staining for Cy-CD8 and FITC-CD11c, the cells were fixed in Cytofix/Cytoperm solution (BD Pharmingen; BD Biosciences) for 30 min at 4°C and stained with PE-conjugated anti-mouse IFN- $\gamma$  for 30 min at 4°C (cat. no. 562333; BD Biosciences). Finally, they were analyzed on a FACSCanto™ II (BD Biosciences) with FlowJo v10 software.

**Cytokine analysis.** Splenocytes ( $2 \times 10^6$ ) were stimulated with CD3 mAb (0.1  $\mu$ g/ml), anti-4-1BB mAb (5  $\mu$ g/ml) and ISTF (10  $\mu$ g/ml). After 48 h of incubation, culture supernatants were collected. The cytokines in the culture supernatants were quantified using a cytometric bead array kit (BD Biosciences), according to the manufacturer's protocol. They were analyzed on a FACSCanto™ II (BD Biosciences) with FlowJo v10 software.

**Statistical analysis.** All experiments were conducted at least three times, and the data are presented as the mean  $\pm$  standard error of the mean. All the data were analyzed using GraphPad Prism 9 (GraphPad Software, Inc.). Statistical analyses were performed using one-way ANOVA with Tukey's post hoc test, and Shapiro-Wilk test was performed as a test of normality. Survival analysis was performed using the Kaplan-Meier method; the log-rank test was used to determine statistical significance.  $P < 0.05$  was considered to indicate a statistically significant difference.

## Results

**Combined therapy with ISTF and anti-4-1BB mAb eradicates Renca tumors.** To observe whether combined therapy with ISTF and anti-4-1BB mAb could eradicate Renca tumors, mice were treated with 100  $\mu$ g ISTF and 100  $\mu$ g anti-4-1BB mAb. Mice inoculated with Renca tumors were injected with ISTF on days 3, 7 and 12 with anti-4-1BB mAb on days 7 and 12, while the control group received PBS and rat IgG. The tumors in the control mice grew, and these mice died from tumor overgrowth by day 37. The tumor growth of the 4-1BB-mono-treated mice was slower than that of the control mice, but the ISTF-mono-treated group was similar to the control group; i.e., ISTF mono-treatment was ineffective. The combined treatment of mice with ISTF and agonistic 4-1BB antibody had a greater antitumor effect than ISTF or anti-4-1BB mAb alone, and 50% of mice showed partial tumor regression between days 12 and 17 (Fig. 1A and B). In addition, ISTF alone or 4-1BB alone, or 4-1BB and ISTF co-administration did not induce liver toxicity, as indicated by the levels of ALT and AST (Fig. 1C). The control and ISTF monotherapy mice all died between days 31 and 37 after tumor cell inoculation. Monotherapy with anti-4-1BB mAb showed modest antitumor effects. The anti-4-1BB mAb monotherapy group had slower tumor growth and survived longer than the control group, but eventually, these mice died between 37 and 43 days. ISTF and anti-4-1BB mAb co-treatment notably inhibited tumor growth (Fig. 1A) and increased the mouse survival time compared with the other experimental groups. A total of 50% of the ISTF and anti-4-1BB mAb co-treated mice survived until the end of the experiment (Fig. 1D).

**ISTF and anti-4-1BB mAb co-treatment induces marked expansion of CD11c<sup>+</sup>CD8<sup>+</sup> cells in splenocytes of tumor-bearing mice.** To analyze the relationship between tumor regression and immune cell populations, the cell populations in the spleens of mice bearing the Renca tumors were analyzed. As shown in Fig. 1A, ISTF and 4-1BB co-treatment almost removed the tumor ~day 17. Thus, on day 14 after Renca tumor cell inoculation, spleens were harvested by sacrificing the mice, and the percentage of CD3<sup>+</sup>CD4<sup>+</sup> T cells, CD3<sup>+</sup>CD8<sup>+</sup> T cells, B220<sup>+</sup> B cells, CD3<sup>+</sup>DX5<sup>+</sup> natural killer (NK) cells, CD11b<sup>+</sup>F480<sup>+</sup> macrophages, CD4<sup>+</sup>Fox3<sup>+</sup> Treg cells and CD11c<sup>+</sup>CD8<sup>+</sup> T cells were analyzed by FACS. The proportion of CD3<sup>+</sup>CD8<sup>+</sup> T cells in the ISTF + 4-1BB group was significantly higher than that in the control mice, but comparable to that in the 4-1BB-mono-therapy mice (Figs. 2A and S1A). The percentage of CD11c<sup>+</sup>CD8<sup>+</sup> T cells in the ISTF + 4-1BB group showed the most prominent increase compared with that for either treatment alone. These cells constituted 18% of the total spleen cells of the ISTF and anti-4-1BB mAb co-treated mice, but only 1.1% of those of the control IgG and PBS-treated mice. The percentage of CD11c<sup>+</sup>CD8<sup>+</sup> cells in the anti-4-1BB mAb monotherapy group was 4.9%, higher than that in the control group, but lower than that in the ISTF + 4-1BB group. Even with 4-1BB treatment alone, the percentage of CD11c<sup>+</sup>CD8<sup>+</sup> cells increased 4.5-fold compared with the control group, but the increase was an 16-fold increase in the ISTF + 4-1BB group compared with the control group (Figs. 2B and S1B). The percentages of CD4<sup>+</sup>Fox3<sup>+</sup> Treg cells (Figs. 2C and S1C), CD11b<sup>+</sup>F480<sup>+</sup> macrophages (Figs. 2D and S2D), CD3<sup>+</sup>CD4<sup>+</sup> T cells (Figs. 2E and S1E), CD3<sup>+</sup>DX5<sup>+</sup> NK cells (Figs. 2F and S1F) and



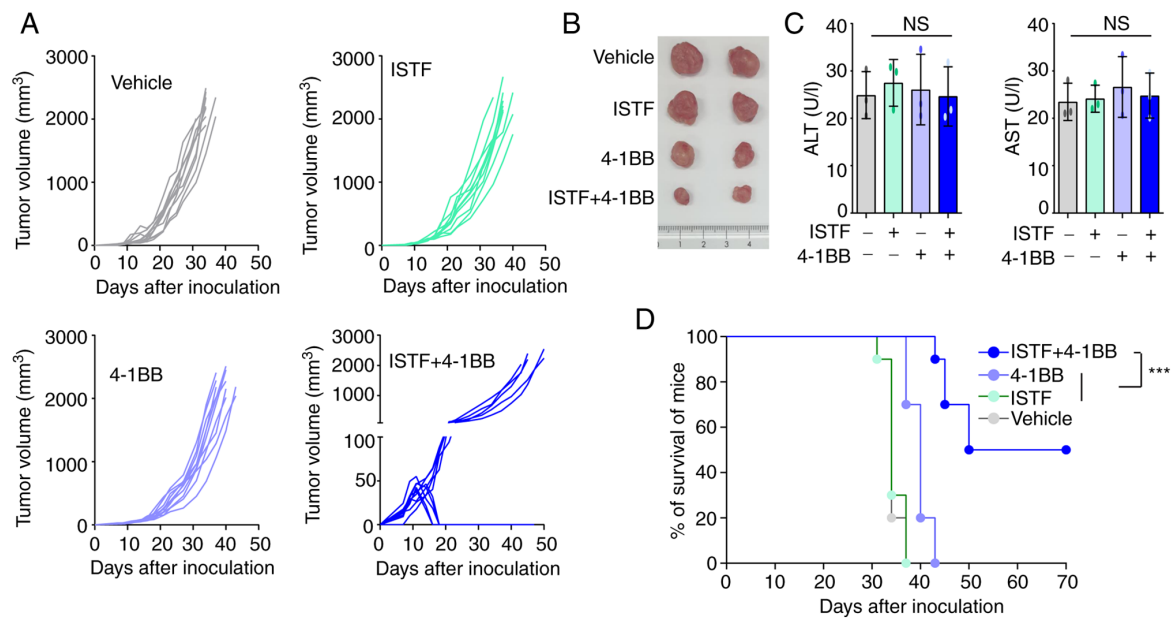


**Figure 1.** Combined therapy with ISTF and anti-4-1BB mAb has antitumor effects in mice inoculated with Renca cells. Mice were inoculated with Renca tumor cells on day 0. Tumor-bearing mice were divided into four groups and treated with the following reagents: i) PBS and control mAb (rat IgG); ii) ISTF monotherapy; iii) 4-1BB mAb monotherapy; and iv) ISTF and 4-1BB mAb combined. Mice were subcutaneously injected with Renca tumor cells ( $1 \times 10^6$ /mouse). ISTF (100  $\mu$ g/mouse) was injected i.p. on days 3, 7 and 12, and anti-4-1BB mAb (100  $\mu$ g/mouse) was injected i.p. on days 7 and 12, while a control group received PBS and/or rat IgG, respectively. Tumor diameter was measured every 2-3 days, and tumor volume (in  $\text{mm}^3$ ) was calculated using a caliper. Tumor size was expressed as tumor volume based on the following formula: Tumor volume ( $\text{mm}^3$ ) = (major axis)  $\times$  (minor axis)  $\times$  (height)  $\times 0.52$ . (A) Effect of combined therapy with ISTF and anti-4-1BB mAb on Renca tumor volume. Each line indicates the tumor volume of the individual animal. Results shown are representative of three independent experiments. n, number of mice per experiment. (B) Representative images of tumors on days 21 in the same condition as (A). (C) Serum ALT and AST were measured. (D) Survival rate of mice was determined. The animals were sacrificed when the longest dimensions of the tumors were  $>20$  mm. Comparison of survival curves with log-rank test yielded a statistical significance of \*\*\* $P < 0.001$ . NS, not significant; ISTF, immunostimulatory factor; mAb, monoclonal antibody; i.p., intraperitoneally; ALT, alanine aminotransferase; AST, aspartate aminotransferase.

CD11b<sup>+</sup>Gr1<sup>+</sup>T cells (Figs. 2G and S1G) showed no significant differences between groups. However, the percentage of B220<sup>+</sup> B cells (Figs. 2H and S1H) was decreased in the ISTF + 4-1BB group compared with the control group. These results showed that combination therapy with ISTF and anti-4-1BB mAb had a synergistic effect on the increase in CD8<sup>+</sup>CD11c<sup>+</sup> T cells in tumor-bearing mice.

*Combined therapy with ISTF and anti-4-1BB mAb induces a greater increase in the number of tumor-reactive effector cells than suppressor cells.* As shown in the image in Fig. 3A, the sizes of the spleens and TDLNs of the mice in the ISTF + 4-1BB group were larger than those in the other experimental groups. Consistent with this, the number of splenocytes in the ISTF + 4-1BB group was also significantly higher than in the other experimental groups. On the other hand, the number of splenocytes in the 4-1BB-treated mice was higher than that in the control, but the number of cells in the ISTF-treated group was similar to that in the control (Fig. 3B). Subsequent detailed analysis of the immune cell subpopulations revealed that the number of CD11c<sup>+</sup>CD8<sup>+</sup> T cells in the ISTF + 4-1BB group was significantly increased compared with the other groups (Fig. 3C). The numbers of CD3<sup>+</sup>CD4<sup>+</sup> T cells (Fig. 3D) and CD3<sup>+</sup>CD8<sup>+</sup> T cells (Fig. 3E) increased in the ISTF + 4-1BB group compared with the control and ISTF groups, but were similarly increased in the 4-1BB group. The numbers of CD3<sup>+</sup>DX5<sup>+</sup> NK cells (Fig. 3F), CD11b<sup>+</sup>F480<sup>+</sup> macrophages (Fig. 3G), and B220<sup>+</sup> B cells (Fig. 3H) were similar between the groups. The numbers of CD11b<sup>+</sup>Gr1<sup>+</sup>T cells (Fig. 3I) and CD4<sup>+</sup>Foxp3<sup>+</sup> cells (Fig. 3J)

increased in the ISTF + 4-1BB group compared with the control and ISTF groups, however, there were no significant differences compared with the 4-1BB administration group. The ratio of tumor-reactive immune cells to suppressor cells has been shown to be more important than the density or total number of each subtype for antitumor immune responses in human and animal models (31-33). Therefore, the present study next investigated the ratios of CD4<sup>+</sup>Foxp3<sup>+</sup> cells and CD11b<sup>+</sup>Gr1<sup>+</sup>T cells, which are considered regulatory T cells and myeloid-derived suppressor cells, respectively (31,34,35), to CD8<sup>+</sup> T cells and CD11c<sup>+</sup>CD8<sup>+</sup> T cells. The CD3<sup>+</sup>CD8<sup>+</sup> cell/CD4<sup>+</sup>Foxp3<sup>+</sup> cell, CD3<sup>+</sup>CD8<sup>+</sup> cell/CD11b<sup>+</sup>Gr1<sup>+</sup>T cell, CD11c<sup>+</sup>CD8<sup>+</sup> cell/CD4<sup>+</sup>Foxp3<sup>+</sup> cell, and CD11c<sup>+</sup>CD8<sup>+</sup> cell/CD11b<sup>+</sup>Gr1<sup>+</sup>T cell ratios were increased 2.8-, 2.6-, 13.6- and 11.3-fold, respectively, in the ISTF + 4-1BB group, compared with the control group (Fig. 3K-N). This indicated that combined therapy with ISTF and anti-4-1BB mAb led to a greater increase in the number of tumor-reactive effector cells than suppressor cells.

*Combined therapy with ISTF and anti-4-1BB mAb induces marked expansion of CD11c<sup>+</sup>CD8<sup>+</sup> cells in TILs.* We previously reported that CD11c<sup>+</sup>CD8<sup>+</sup> T cells play a role in antitumor immunity in melanoma mouse models (36). The administration of anti-4-1BB mAb to B16F10-melanoma-bearing mice can induce the marked expansion of CD11c<sup>+</sup>CD8<sup>+</sup> T cells in parallel with the suppression of pulmonary tumors (37). As CD11c<sup>+</sup>CD8<sup>+</sup> T cells express high levels of CD107a, a marker of activated cytotoxic T lymphocytes (CTLs), they have been suggested to be cells with a role in the antitumor immunity



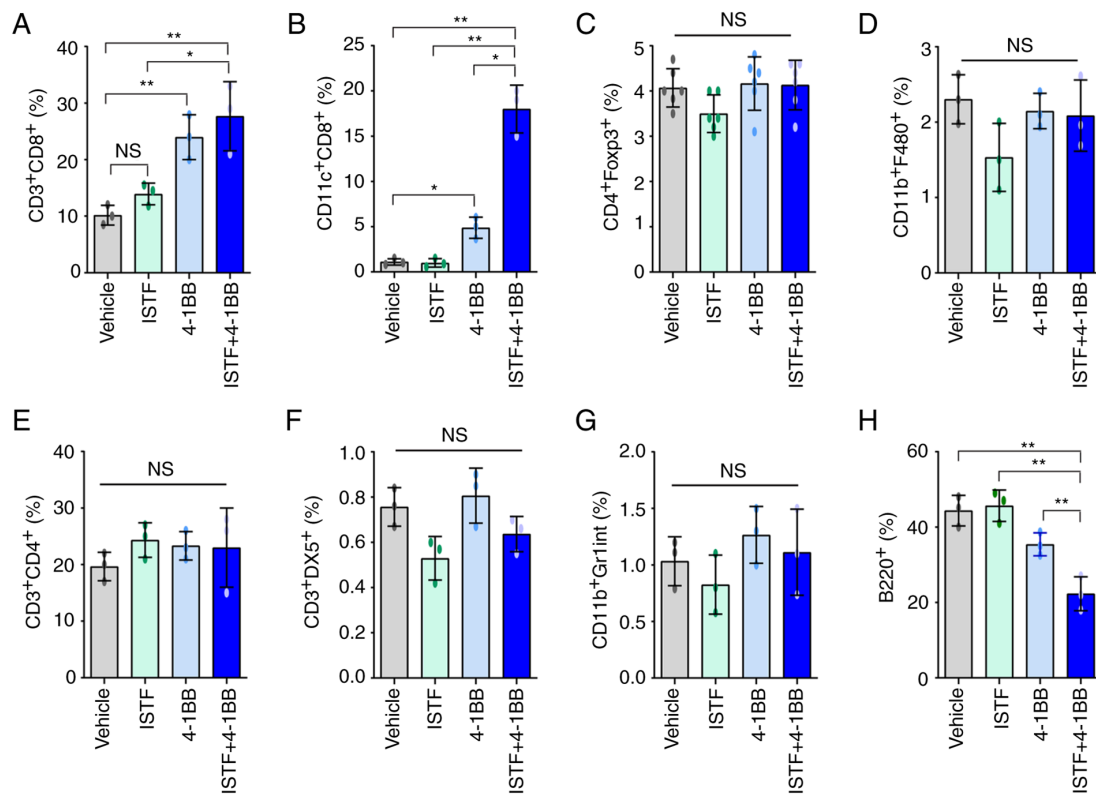


Figure 2. ISTF and anti-4-1BB mAb co-treatment induces marked expansion of CD11c<sup>+</sup>CD8<sup>+</sup> T cells in splenocytes of tumor-bearing mice. Renca tumors were established and four groups of mice were treated with ISTF and/or anti-4-1BB mAb as described in Fig. 1. On day 14, splenocytes were excised; double stained with PE-, Cy- and FITC-conjugated antibodies and analyzed by fluorescence activated cell sorting. Bar charts indicating the proportions of (A) CD3<sup>+</sup>CD8<sup>+</sup> T cells, (B) CD11c<sup>+</sup>CD8<sup>+</sup> T cells, (C) CD4<sup>+</sup>Foxp3<sup>+</sup> Treg cells, (D) CD11b<sup>+</sup>F480<sup>+</sup> macrophages, (E) CD3<sup>+</sup>CD4<sup>+</sup> T cells, (F) CD3<sup>+</sup>DX5<sup>+</sup> natural killer cells, (G) CD11b<sup>+</sup>Gr1<sup>int</sup> myeloid cells and (H) B220<sup>+</sup> B cells. Data are presented as the mean ± SD (n=3). \*P<0.05 and \*\*P<0.01. NS, not significant; ISTF, immunostimulatory factor; mAb, monoclonal antibody.

induced by anti-4-1BB mAb (36). In addition, CD8<sup>+</sup> T cells in TILs are considered critical immune effector cells for antitumor immune responses (3). This prompted the present study to analyze CD8<sup>+</sup> T cells and CD11c<sup>+</sup>CD8<sup>+</sup> T cells in TILs. TILs from the tumors of each type of mouse were purified and characterized. The TILs mainly consisted of CD4<sup>+</sup> T cells, CD8<sup>+</sup> T cells, and CD11c<sup>+</sup>CD8<sup>+</sup> T cells. The percentages of CD3<sup>+</sup>CD4<sup>+</sup> T cells were similar between the groups (Figs. 4A and S2). The percentages and numbers of CD3<sup>+</sup>CD8<sup>+</sup> T cells (Fig. 4B) and CD11c<sup>+</sup>CD8<sup>+</sup> T cells (Fig. 4C) showed greater increases in the ISTF + 4-1BB group than in the other experimental groups. The in the ISTF + 4-1BB group had the highest numbers of TIL cells per mg of tumor compared with the other groups (Fig. 4D). As the difference in tumor size between the ISTF + 4-1BB group and control group may have affected the number and frequency of TIL subtypes in tumors, the number of TIL subtypes in the same amounts of tumor tissue were compared. The numbers of CD3<sup>+</sup>CD4<sup>+</sup> T cells, CD3<sup>+</sup>CD8<sup>+</sup> T cells and CD11c<sup>+</sup>CD8<sup>+</sup> T cells per mg of tumor tissue were 2.7-, 11.1-, 32.3-fold higher, respectively, in the ISTF + 4-1BB group than in the control group (Fig. 4E-G).

*CD11c<sup>+</sup>CD8<sup>+</sup> T cells increased by combination therapy with ISTF and anti-4-1BB mAb have high IFN-γ production ability.* The next goal was to determine whether the significant increases in CD8<sup>+</sup> T cells and CD11c<sup>+</sup>CD8<sup>+</sup> T cells induced by anti-4-1BB mAb and ISTF co-administration resulted in

antitumor activity. IFN-γ has been considered to be a key cytokine in tumor immunity (38). To further clarify the mechanisms underlying the ISTF- and 4-1BB-mediated antitumor immunity in our model, IFN-γ production in CD8<sup>+</sup> T cells and CD11c<sup>+</sup>CD8<sup>+</sup> T cells was investigated by intracellular cytokine staining. As expected, the IFN-γ-producing CD8<sup>+</sup> T cells and CD11c<sup>+</sup>CD8<sup>+</sup> T cells were much higher in the ISTF + 4-1BB group than those in the control mice. IFN-γ-producing CD8<sup>+</sup> T cells constituted 31.9% of the total splenocytes of mice in the ISTF + 4-1BB group, and 5.2 and 18.9% of those in the ISTF or 4-1BB monotherapy groups, respectively (Fig. 5A). Among CD8<sup>+</sup> T cells, the proportion and number of CD11c<sup>+</sup>IFN-γ<sup>+</sup> cells were 10.8-fold or 4.1-fold and 36.4-fold or 6.6-fold higher in the mice in the ISTF + 4-1BB group than the ISTF or 4-1BB monotherapy groups, respectively (Fig. 5B). In the mice in the ISTF + 4-1BB group, 66.7% of the CD8<sup>+</sup>CD11c<sup>+</sup> cells secreted IFN-γ (Fig. 5C). Therefore, a significantly increased number of CD11c<sup>+</sup>CD8<sup>+</sup> T cells, due to anti-4-1BB mAb and ISTF co-administration, had high IFN-γ production activity and represent antitumor effector cells.

*ISTF and anti-4-1BB mAb co-treatment increases the production of inflammatory cytokines.* Studies have shown that the production of pro-inflammatory cytokines can contribute to cancer immunotherapy, acting on every phase of the cancer immune cycle, including improving antigen priming, increasing the number of effector immune cells in

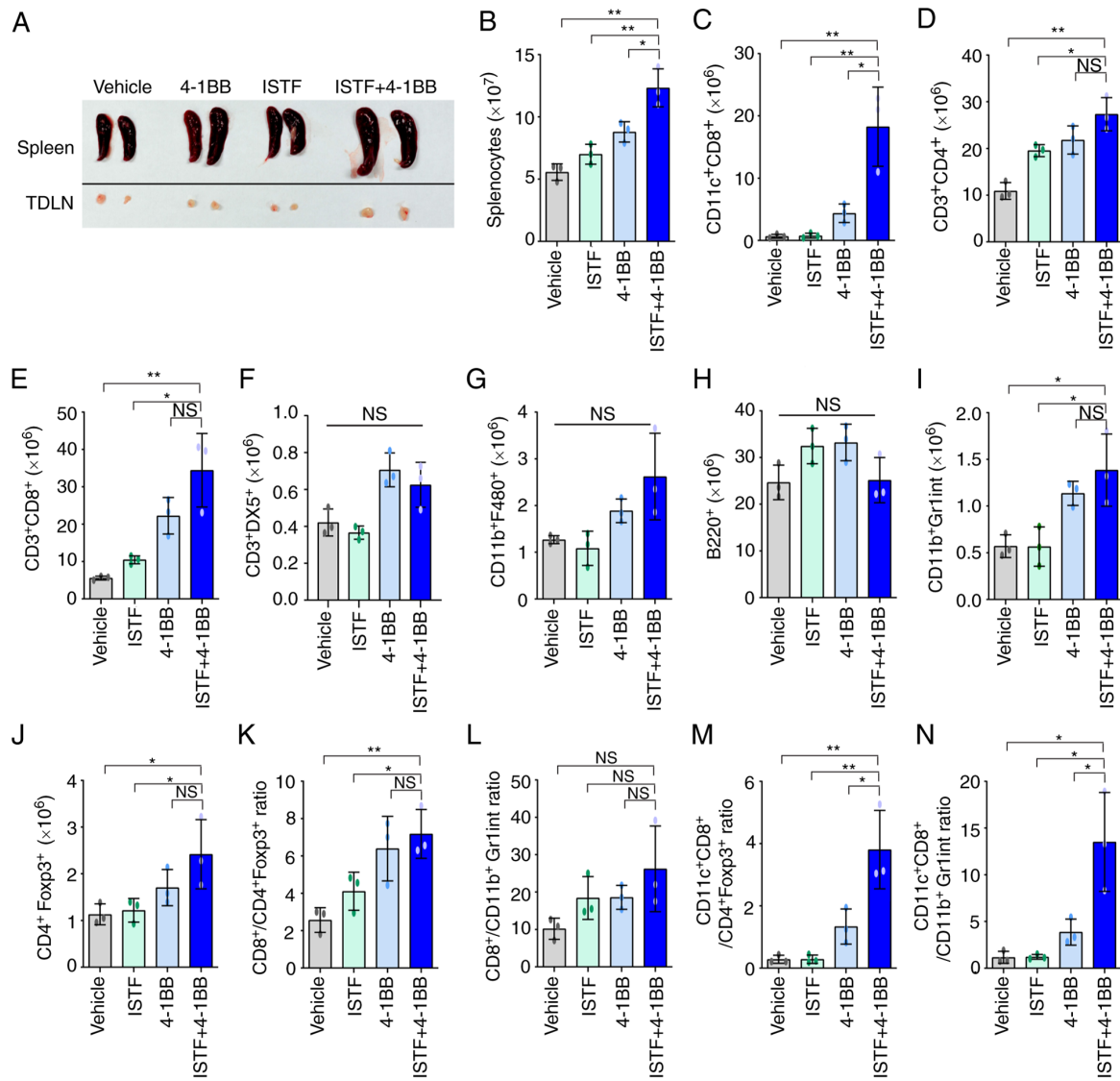


Figure 3. Combined therapy with ISTF and anti-4-1BB mAb leads to a greater increase in the number of tumor-reactive effector cells than suppressor cells. Renca tumors were established and four groups of mice were treated with ISTF and/or anti-4-1BB mAb as described in Fig. 1. On day 14, splenocytes were excised; double stained with PE-, cy and FITC-conjugated antibodies and analyzed by fluorescence activated cell sorting. (A) Representative images of spleen and inguinal TDLNs in each group on day 14. (B) The total numbers of splenocytes were determined on day 14. The numbers of (C) CD11c<sup>+</sup>CD8<sup>+</sup>T cells, (D) CD3<sup>+</sup>CD4<sup>+</sup> T cells, (E) CD3<sup>+</sup>CD8<sup>+</sup> T cells, (F) CD3<sup>+</sup>DX5<sup>+</sup> natural killer cells, (G) CD11b<sup>+</sup> F480<sup>+</sup> cells, (H) B220<sup>+</sup> B cells, (I) CD11b<sup>+</sup>Gr1<sup>int</sup> cells and (J) CD4<sup>+</sup>Foxp3<sup>+</sup> Treg cells. (K) The CD3<sup>+</sup>CD8<sup>+</sup> cell/CD4<sup>+</sup>Foxp3<sup>+</sup> cell, (L) CD3<sup>+</sup>CD8<sup>+</sup> cell/CD11b<sup>+</sup>Gr1<sup>int</sup> cell, (M) CD11c<sup>+</sup>CD8<sup>+</sup> cell/CD4<sup>+</sup>Foxp3<sup>+</sup> cell, and (N) CD11c<sup>+</sup>CD8<sup>+</sup> cell/CD11b<sup>+</sup>Gr1<sup>int</sup> cell ratios were analyzed. Data are presented as the mean  $\pm$  SD (n=3). \*P<0.05 and \*\*P<0.01. NS, not significant; ISTF, immunostimulatory factor; mAb, monoclonal antibody; TDLN, tumor-draining lymph node.

the tumor microenvironment and enhancing their cytolytic activity (39,40). IFN- $\gamma$  is known to play an important role in the anticancer activity of CD8<sup>+</sup> T cells (38,41).

Next, the ability of ISTF and anti-4-1BB mAb combined therapy to directly induce cytokine production was analyzed *in vitro*. Pro-inflammatory cytokines, including IFN- $\gamma$ , were measured in the supernatants of splenocytes from naïve mice stimulated with various combinations of anti-CD3 mAb (0.1  $\mu$ g/ml), anti-4-1BB mAb (5  $\mu$ g/ml) and ISTF (10  $\mu$ g/ml). ISTF, anti-4-1BB mAb and anti-CD3 mAb co-treatment increased the production of IFN- $\gamma$  (Fig. 6A), IL-6 (Fig. 6B) and TNF- $\alpha$  (Fig. 6C). In particular, IFN- $\gamma$  showed a significant synergistic effect compared with the mono-treatment groups (Fig. 6A). The ISTF mono-treatment without stimulation with 4-1BB and CD3 also resulted in increased production of IL-6,

IFN- $\gamma$  and TNF- $\alpha$  compared with the vehicle-treated group, but the levels of IFN- $\gamma$  and IL-6 were significantly lower than that of the co-treatment group (Fig. 6A-C). IL-10 is considered an immunosuppressive cytokine because it can decrease the antigen-presenting activity of dendritic cells (DCs) and inhibit the cytotoxic and cytokine-release functions performed by T and NK lymphocytes (42,43). The level of IL-10 production in the ISTF and 4-1BB co-stimulation group was similar to that in the ISTF and 4-1BB mono-stimulated groups, and there was no significant difference (Fig. 6D).

## Discussion

The present study reported a marked increase in CD11c<sup>+</sup>CD8<sup>+</sup> T cells in response to anti-4-1BB mAb and ISTF co-treatment

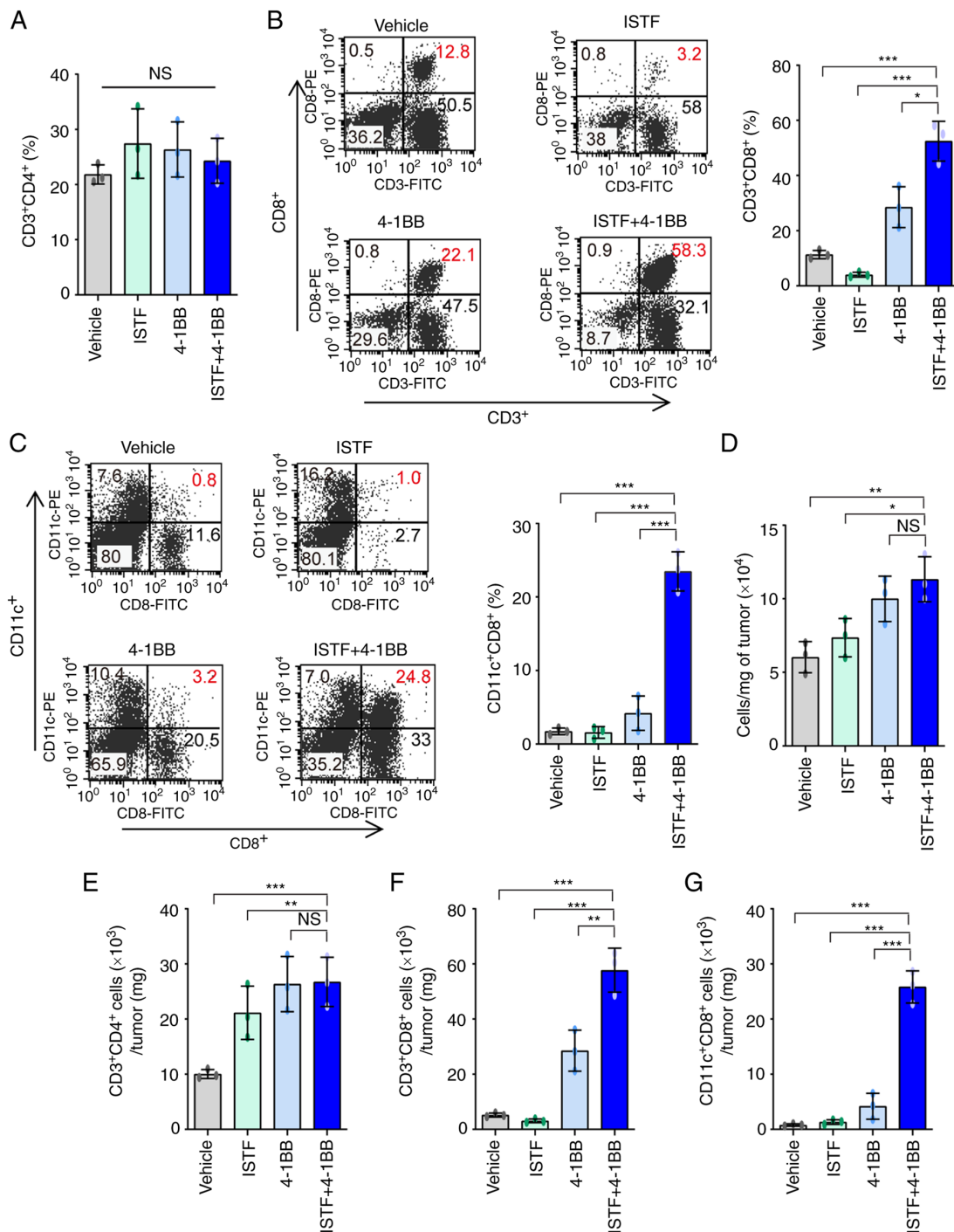


Figure 4. Combined therapy with ISTF and anti-4-1BB mAb induces marked expansion of CD11c<sup>+</sup>CD8<sup>+</sup> T cells in TILs. Renca tumors were established and four groups of mice were treated with ISTF and/or anti-4-1BB mAb as described in Fig. 1. On day 14, the mice were sacrificed and tumors were harvested. TILs were stained with PE, CY and FITC-conjugated antibodies and analyzed by fluorescence activated cell sorting. (A) The % of CD3<sup>+</sup>CD4<sup>+</sup> T cells among TILs. (B) Dot plots show the % of CD3<sup>+</sup>CD8<sup>+</sup> T cells (left panel). Bar chart indicating the proportion of CD3<sup>+</sup>CD8<sup>+</sup> T cells among TILs (right panel). (C) Dot plots show the % of CD11c<sup>+</sup>CD8<sup>+</sup> T cells (left panel). Bar chart indicating the proportion of CD11c<sup>+</sup>CD8<sup>+</sup> T cells among TILs (right panel). (D) The total numbers of TILs per mg of tumors. (E) The number of CD3<sup>+</sup>CD4<sup>+</sup> cells per mg of tumors. (F) The number of CD3<sup>+</sup>CD8<sup>+</sup> cells per mg of tumors. (G) The number of CD11c<sup>+</sup>CD8<sup>+</sup> T cells per mg of tumors. Data are presented as the mean ± SD (n=3). \*P<0.05, \*\*P<0.01 and \*\*\*P<0.001. NS, not significant; ISTF, immunostimulatory factor; mAb, monoclonal antibody; TILs, tumor-infiltrating lymphocytes.

in a tumor model, together with the suppression of tumor growth. ISTF is a component of the bacterial outer membrane, a proteinaceous material distinct from LPS, that can exist in a soluble form and is released by growing and/or lysed bacteria (26). Influenced by the fact that ISTF stimulates APC cells such as macrophages and DCs, the present study

investigated whether ISTF could increase the immunotherapeutic efficiency in the treatment of tumors.

Although cytokine therapy with IL-2 and IFN-γ has been used for advanced RCC, it has only proved efficacious in a limited proportion of patients (16,44). RCC is an immunogenic tumor, based on its response to immunotherapy



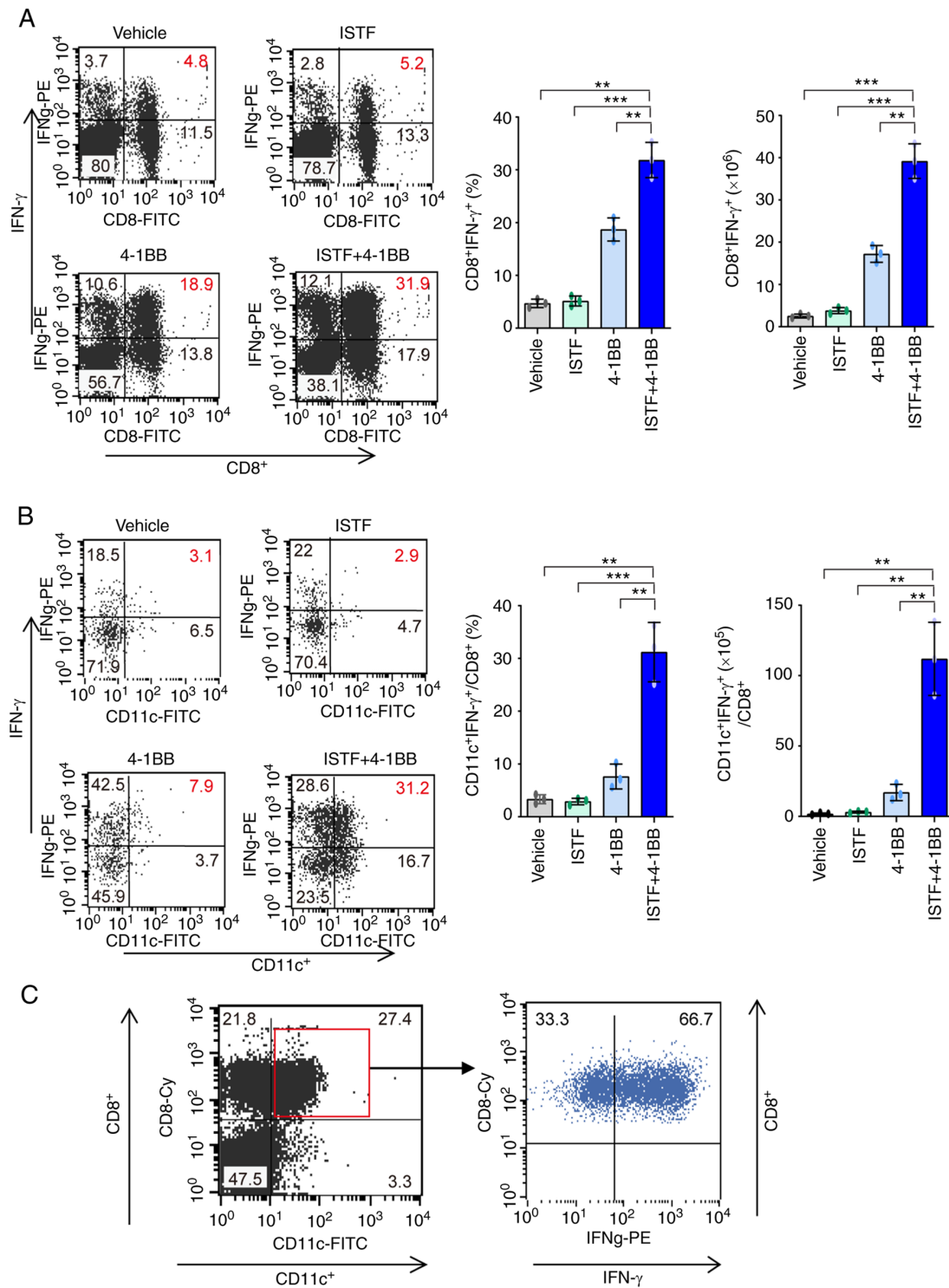


Figure 5. CD11<sup>+</sup>CD8<sup>+</sup> T cells increased by combination therapy with ISTF and anti-4-1BB mAb have high IFN- $\gamma$  production ability. Renca tumors were established and four groups of mice were treated with ISTF and/or anti-4-1BB mAb as described in Fig. 1. To measure the expression of IFN- $\gamma$ , spleens were isolated from Renca-bearing mice on day 14 and cultured with PMA (50 ng/ml) and ionomycin (500 ng/ml); cytokine release was prevented by treatment with Golgi-stop. Following surface staining for FITC-CD8 or Cy-CD8 and FITC-CD11c, the cells were fixed, permeabilized and intracellularly stained with PE-conjugated anti-IFN- $\gamma$ . (A) Dot plots show CD8<sup>+</sup>IFN- $\gamma$ <sup>+</sup> cells (left panel), and the bar chart indicates % of CD8<sup>+</sup>IFN- $\gamma$ <sup>+</sup> cells (middle panel) and the number of CD8<sup>+</sup>IFN- $\gamma$ <sup>+</sup> cells (right panel). (B) Dot plots show CD11c<sup>+</sup>IFN- $\gamma$ <sup>+</sup> cells among CD8<sup>+</sup> cells (left panel). The bar chart indicates % of CD11c<sup>+</sup>IFN- $\gamma$ <sup>+</sup> cells among CD8<sup>+</sup> T cells (middle panel), and the number of CD11c<sup>+</sup>IFN- $\gamma$ <sup>+</sup> cells among CD8<sup>+</sup> T cells (right panel). The cells were first gated on CD8<sup>+</sup> T cells, and the gated cells were analyzed by FACS for CD11c<sup>+</sup>IFN- $\gamma$ <sup>+</sup> cells. (C) Dot plots show IFN- $\gamma$ <sup>+</sup> cells among CD11c<sup>+</sup>CD8<sup>+</sup> T cells. The cells were first gated on CD11c<sup>+</sup>CD8<sup>+</sup> T cells, and the gated cells were analyzed by FACS for IFN- $\gamma$ <sup>+</sup> cells. Data are presented as the mean  $\pm$  SD (n=3). \*\*P<0.01 and \*\*\*P<0.001. ISTF, immunostimulatory factor; mAb, monoclonal antibody; FACS, fluorescence activated cell sorting.

and the increase in tumor T cell infiltration (45). Agonistic mAbs targeting 4-1BB have been developed to harness

4-1BB signaling for cancer immunotherapy (46). 4-1BB, an inducible costimulatory receptor, is transiently expressed

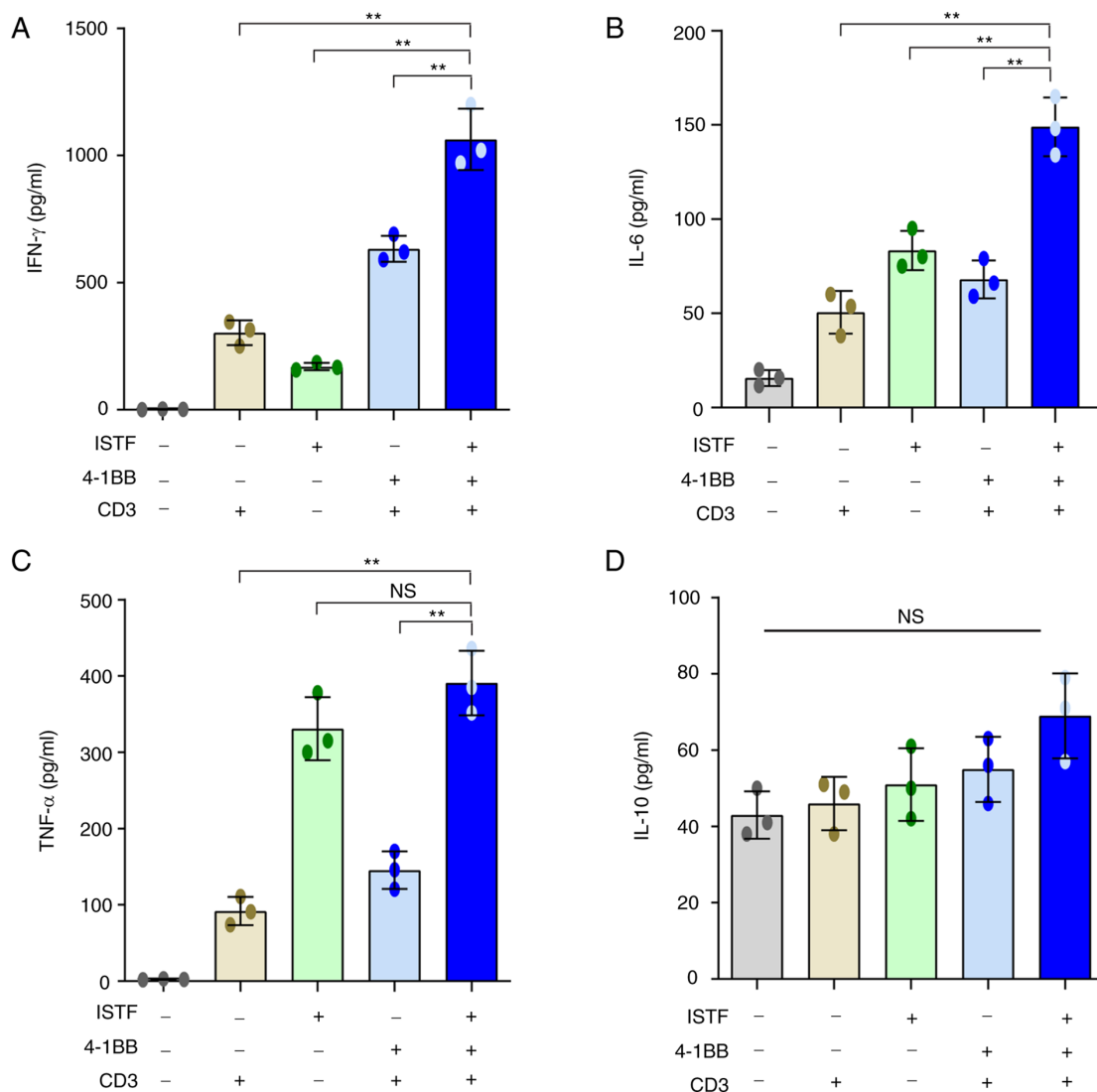


Figure 6. ISTF and anti-4-1BB mAb co-treatment increases the production of inflammatory cytokines. Splenocytes ( $2 \times 10^6$ ) from naïve mice were stimulated with various combinations of anti-CD3 mAb ( $0.1 \mu\text{g/ml}$ ), anti-4-1BB mAb ( $5 \mu\text{g/ml}$ ) and ISTF ( $10 \mu\text{g/ml}$ ). Culture supernatants were collected after 48 h, and the amounts of cytokines in the supernatants were quantified using a cytometric bead array kit on a FACSCanto™ II cytometer equipped with FlowJo v10 software. The concentrations of (A) IFN- $\gamma$ , (B) IL-6, (C) TNF- $\alpha$  and (D) IL-10 in the culture supernatants were measured in pg/ml. Data are presented as the mean  $\pm$  SD (n=3). \*\*P<0.01. NS, not significant; ISTF, immunostimulatory factor; mAb, monoclonal antibody; FACS, fluorescence activated cell sorting.

after T cell receptor engagement on T cells (3). In the tumor micro-environment (TME), 4-1BB activation can enhance the activity of tumor-specific CTLs (47,48). In the present study, anti-4-1BB mAb monotherapy caused slower tumor growth and longer survival compared with the control group. Further studies should be performed to address the mechanism underlying this effect, but we suggest that it was due to the increase of myeloid-derived suppressor cells, regulatory T cells and TGF- $\alpha$  in TME (49,50). Previously, anti-4-1BB mAb, urelumab (IgG4), showed hepatotoxicity at high doses ( $\geq 1 \text{ mg/kg}$ ), but was demonstrated to be safe at  $0.1 \text{ mg/kg}$  every 3 weeks (51). In addition, utomilumab (IgG2) has been found to activate 4-1BB through Fc-mediated crosslinking and shows weaker agonist activity than urelumab (52,53). The modest antitumor activity of utomilumab is better tolerated by patients as monotherapy (51), and no synergistic effects with PD-1 blockade in combination therapy (54). Thus, to reduce adverse effects and improve the antitumor activity of 4-1BB,

it has been identified that bispecific antibody (MCLA-145) can activate 4-1BB without crosslinking via engagement of PD-L1 to enhance tumor-specific T cell response (55). Therefore, it was hypothesized in the current study that a combination of ISTF, promoting antigen presentation and anti-4-1BB mAb, stimulating T cell co-stimulation signals, could increase T cell activity to eradicate RCC. It was found that a combined treatment of mice with ISTF and agonistic 4-1BB antibody increased the antitumor effects and CD11c $^+$ CD8 $^+$  T cells than just ISTF or anti-4-1BB mAb alone. Additionally, most of the CD11c $^+$ CD8 $^+$  T cells were effector cells that produced IFN- $\gamma$ , which is very important for anticancer activity. It was also confirmed *in vitro* that ISTF and 4-1BB stimulation increased IFN- $\gamma$  production in T cells. In addition, ISTF, anti-4-1BB mAb and anti-CD3 mAb co-treatment showed increased synergistic effects on IFN- $\gamma$  compared with the effects in the mono-treatment groups.

Consistent with our previous report (36), Takeda *et al* (56) and Choi *et al* (57) also demonstrated that CD11c $^+$ CD8 $^+$

T cells are effectors of anti-4-1BB-mediated tumor suppression through the induction of Ag-specific CD8<sup>+</sup> T cells and an increase in IFN- $\gamma$ -producing ability, which represents an active phenotype of the effector CTLs. The increase in CD11c expression in CD8<sup>+</sup> T cells can be induced by various immunological stimuli, such as microbial infections or Ag and agonistic anti-4-1BB mAb (58). The level of CD11c expression in CD8<sup>+</sup> T cells can be a useful marker for the evaluation of the degree of expansion and the quality of tumor-specific CTLs as well as a marker for predicting the efficacy of anti-tumor immunotherapies (56). As such, CD11c<sup>+</sup>CD8<sup>+</sup> T cells have been considered effector cells that play a role in the antitumor immunity induced upon stimulation with Ag and anti-4-1BB mAbs. The ultimate goal of cancer immunotherapies is to establish large numbers of effector T cells that have potent antitumor activity. Although ISTF alone did not show anticancer activity in the present study, it showed anticancer activity when co-administered with anti-4-1BB mAb. Thus, it was suggested that it may be used as an adjuvant agent for anticancer immunotherapy.

These results indicated that a combination of ISTF and anti-4-1BB mAb eradicated established tumors by the marked expansion of CD11c<sup>+</sup>CD8<sup>+</sup> T cells with anticancer activity in tumor-bearing mice; therefore, it could be a useful strategy by which to target both antigen presentation and T cell co-stimulatory signals in incurable RCC.

## Acknowledgements

Not applicable.

## Funding

This research was supported by the Basic Science Research Program through the National Research Foundation of Korea (NRF), funded by the Ministry of Education (grant nos. NRF-2017R1D1A1B03036287, NRF-2017R1D1A1B03032831, NRF-2014R1A6A1030318 and NRF-2015R1D1A1A01059994).

## Availability of data and materials

All data generated or analyzed during this study are included in this published article.

## Authors' contributions

SAJ, HTC, WGA and BSK were responsible for the conceptualization of the present study. SAJ, SMP and YJ acquired, analyzed and interpreted the data. SAJ, SMP and YJ confirm the authenticity of all the raw data. SAJ, HTC, WGA and BSK provided the resources. SAJ, YJ, HTC, WGA and BSK wrote, reviewed and edited the manuscript, and gave the final approval of the manuscript. All authors have read and approved the final manuscript.

## Ethics approval and consent to participate

Animal studies were approved by the University of Ulsan Animal Care and Use Committee (approval no. HTC-14-030; Nam-gu, Republic of Korea).

## Patient consent for publication

Not applicable.

## Competing interests

The authors declare that they have no competing interests.

## References

- Vitale MG and Carteni G: Recent developments in second and third line therapy of metastatic renal cell carcinoma. *Expert Rev Anticancer Ther* 16: 469-471, 2016.
- Makhov P, Joshi S, Ghatalia P, Kutikov A, Uzzo RG and Kolenko VM: Resistance to systemic therapies in clear cell renal cell carcinoma: Mechanisms and management strategies. *Mol Cancer Ther* 17: 1355-1364, 2018.
- Bartkowiak T and Curran MA: 4-1BB Agonists: Multi-potent potentiators of tumor immunity. *Front Oncol* 5: 117, 2015.
- Yagoda A, Abi-Rached B and Petrylak D: Chemotherapy for advanced renal-cell carcinoma: 1983-1993. *Semin Oncol* 22: 42-60, 1995.
- Reeves DJ and Liu CY: Treatment of metastatic renal cell carcinoma. *Cancer Chemother Pharmacol* 64: 11-25, 2009.
- Hah YS and Koo KC: Immunology and immunotherapeutic approaches for advanced renal cell carcinoma: A comprehensive review. *Int J Mol Sci* 22: 4452, 2021.
- Brown LC, Desai K, Zhang T and Ornstein MC: The immunotherapy landscape in renal cell carcinoma. *BioDrugs* 34: 733-748, 2020.
- Considine B and Hurwitz ME: Current status and future directions of immunotherapy in renal cell carcinoma. *Curr Oncol Rep* 21: 34, 2019.
- Negrier S, Escudier B, Lasset C, Douillard JY, Savary J, Chevreau C, Ravaud A, Mercatello A, Peny J, Mousseau M, *et al*: Recombinant human interleukin-2, recombinant human interferon alfa-2a, or both in metastatic renal-cell carcinoma. *Groupe Francais d'Immunotherapie. N Engl J Med* 338: 1272-1278, 1998.
- Sica G and Chen L: Modulation of the immune response through 4-1BB. *Adv Exp Med Biol* 465: 355-362, 2000.
- Vinay DS and Kwon BS: Role of 4-1BB in immune responses. *Semin Immunol* 10: 481-489, 1998.
- Melero I, Shuford WW, Newby SA, Aruffo A, Ledbetter JA, Hellström KE, Mittler RS and Chen L: Monoclonal antibodies against the 4-1BB T-cell activation molecule eradicate established tumors. *Nat Med* 3: 682-685, 1997.
- Miller RE, Jones J, Le T, Whitmore J, Boiani N, Gliniak B and Lynch DH: 4-1BB-specific monoclonal antibody promotes the generation of tumor-specific immune responses by direct activation of CD8 T cells in a CD40-dependent manner. *J Immunol* 169: 1792-1800, 2002.
- Taraban VY, Rowley TF, O'Brien L, Chan HT, Haswell LE, Green MH, Tutt AL, Glennie MJ and Al-Shamkhani A: Expression and costimulatory effects of the TNF receptor superfamily members CD134 (OX40) and CD137 (4-1BB), and their role in the generation of anti-tumor immune responses. *Eur J Immunol* 32: 3617-3627, 2002.
- Wilcox RA, Flies DB, Zhu G, Johnson AJ, Tamada K, Chapoval AI, Strome SE, Pease LR and Chen L: Provision of antigen and CD137 signaling breaks immunological ignorance, promoting regression of poorly immunogenic tumors. *J Clin Invest* 109: 651-659, 2002.
- Ju SA, Cheon SH, Park SM, Tam NQ, Kim YM, An WG and Kim BS: Eradication of established renal cell carcinoma by a combination of 5-fluorouracil and anti-4-1BB monoclonal antibody in mice. *Int J Cancer* 122: 2784-2790, 2008.
- Wallin JJ, Bendell JC, Funke R, Sznol M, Korski K, Jones S, Hernandez G, Mier J, He X, Hodi FS, *et al*: Atezolizumab in combination with bevacizumab enhances antigen-specific T-cell migration in metastatic renal cell carcinoma. *Nat Commun* 7: 12624, 2016.
- McDermott DF, Sosman JA, Sznol M, Massard C, Gordon MS, Hamid O, Powderly JD, Infante JR, Fassò M, Wang YV, *et al*: Atezolizumab, an Anti-programmed death-ligand 1 antibody, in metastatic renal cell carcinoma: Long-term safety, clinical activity, and immune correlates from a phase Ia study. *J Clin Oncol* 34: 833-842, 2016.



19. Zizzari IG, Napoletano C, Di Filippo A, Botticelli A, Gelibter A, Calabrò F, Rossi E, Schinzari G, Urbano F, Pomati G, *et al*: Exploratory pilot study of circulating biomarkers in metastatic renal cell carcinoma. *Cancers (Basel)* 12: 2620, 2020.
20. Li Y, Wang Z, Jiang W, Zeng H, Liu Z, Lin Z, Qu Y, Xiong Y, Wang J, Chang Y, *et al*: Tumor-infiltrating TNFRSF9 + CD8 + T cells define different subsets of clear cell renal cell carcinoma with prognosis and immunotherapeutic response. *Oncoimmunology* 9: 1838141, 2020.
21. Bromley GS and Solender M: Hand infection caused by *Actinobacillus actinomycetemcomitans*. *J Hand Surg Am* 11: 434-436, 1986.
22. Hofstad T and Stallemo A: Subacute bacterial endocarditis due to *Actinobacillus actinomycetemcomitans*. *Scand J Infect Dis* 13: 78-79, 1981.
23. Patel PK and Seitchik MW: *Actinobacillus actinomycetemcomitans*: A new cause for granuloma of the parotid gland and buccal space. *Plast Reconstr Surg* 77: 476-478, 1986.
24. Salman RA, Bonk SJ, Salman DG and Glickman RS: Submandibular space abscess due to *Actinobacillus actinomycetemcomitans*. *J Oral Maxillofac Surg* 44: 1002-1005, 1986.
25. Weir DM and Blackwell CC: Interaction of bacteria with the immune system. *J Clin Lab Immunol* 10: 1-12, 1983.
26. Jeong SJ, Yee ST, Jo WS, Yu SH, Lee SH, Lim YJ, Yoo YH, Kim JM, Lee JD and Jeong MH: A novel factor isolated from *Actinobacillus actinomycetemcomitans* stimulates mouse B cells and human peripheral blood mononuclear cells. *Infect Immun* 68: 5132-5138, 2000.
27. Jo WS, Yee ST, Yoon S, Nam BH, Do E, Jung BS, Jeong SJ, Hong SH, Yoo YH, Kang CD, *et al*: Immunostimulating factor isolated from *Actinobacillus actinomycetemcomitans* stimulates monocytes and inflammatory macrophages. *Microbiol Immunol* 50: 535-542, 2006.
28. Cheuk AT, Mufti GJ and Guinn BA: Role of 4-1BB:4-1BB ligand in cancer immunotherapy. *Cancer Gene Ther* 11: 215-226, 2004.
29. Schwartz RH: T cell anergy. *Annu Rev Immunol* 21: 305-334, 2003.
30. Ju SA, Lee SC, Kwon TH, Heo SK, Park SM, Paek HN, Suh JH, Cho HR, Kwon B, Kwon BS and Kim BS: Immunity to melanoma mediated by 4-1BB is associated with enhanced activity of tumour-infiltrating lymphocytes. *Immunol Cell Biol* 83: 344-351, 2005.
31. Shen Z, Zhou S, Wang Y, Li RL, Zhong C, Liang C and Sun Y: Higher intratumoral infiltrated Foxp3+ Treg numbers and Foxp3+/CD8+ ratio are associated with adverse prognosis in resectable gastric cancer. *J Cancer Res Clin Oncol* 136: 1585-1595, 2010.
32. Sato E, Olson SH, Ahn J, Bundy B, Nishikawa H, Qian F, Jungbluth AA, Frosina D, Gnjatich S, Ambrosone C, *et al*: Intraepithelial CD8+ tumor-infiltrating lymphocytes and a high CD8+/regulatory T cell ratio are associated with favorable prognosis in ovarian cancer. *Proc Natl Acad Sci USA* 102: 18538-18543, 2005.
33. Ju SA, Park SM, Lee YS, Bae JH, Yu R, An WG, Suh JH and Kim BS: Administration of 6-gingerol greatly enhances the number of tumor-infiltrating lymphocytes in murine tumors. *Int J Cancer* 130: 2618-2628, 2012.
34. Sarkar R, Mathew A and Sehrawat S: Myeloid-derived suppressor cells confer infectious tolerance to dampen virus-induced tissue immunoinflammation. *J Immunol* 203: 1325-1337, 2019.
35. Obregon-Henao A, Henao-Tamayo M, Orme IM and Ordway DJ: Gr1(int)CD11b+ myeloid-derived suppressor cells in *Mycobacterium tuberculosis* infection. *PLoS One* 8: e80669, 2013.
36. Ju SA, Park SM, Lee SC, Kwon BS and Kim BS: Marked expansion of CD11c+CD8+ T-cells in melanoma-bearing mice induced by anti-4-1BB monoclonal antibody. *Mol Cells* 24: 132-138, 2007.
37. Kim SH, Singh R, Han C, Cho E, Kim YI, Lee DG, Kim YH, Kim SS, Shin DH, You HJ, *et al*: Chronic activation of 4-1BB signaling induces granuloma development in tumor-draining lymph nodes that is detrimental to subsequent CD8+ T cell responses. *Cell Mol Immunol* 18: 1956-1968, 2021.
38. Castro F, Cardoso AP, Gonçalves RM, Serre K and Oliveira MJ: Interferon-gamma at the crossroads of tumor immune surveillance or evasion. *Front Immunol* 9: 847, 2018.
39. Chen DS and Mellman I: Oncology meets immunology: The cancer-immunity cycle. *Immunity* 39: 1-10, 2013.
40. Chen DS and Mellman I: Elements of cancer immunity and the cancer-immune set point. *Nature* 541: 321-330, 2017.
41. Bhat P, Leggett G, Waterhouse N and Frazer IH: Interferon-gamma derived from cytotoxic lymphocytes directly enhances their motility and cytotoxicity. *Cell Death Dis* 8: e2836, 2017.
42. Llopiz D, Ruiz M, Infante S, Villanueva L, Silva L, Hervas-Stubbs S, Alignani D, Guruceaga E, Lasarte JJ and Sarobe P: IL-10 expression defines an immunosuppressive dendritic cell population induced by antitumor therapeutic vaccination. *Oncotarget* 8: 2659-2671, 2017.
43. Moore KW, de Waal Malefyt R, Coffman RL and O'Garra A: Interleukin-10 and the interleukin-10 receptor. *Annu Rev Immunol* 19: 683-765, 2001.
44. Motzer RJ, Bander NH and Nanus DM: Renal-cell carcinoma. *N Engl J Med* 335: 865-875, 1996.
45. Vuong L, Kotecha RR, Voss MH and Hakimi AA: Tumor micro-environment dynamics in clear-cell renal cell carcinoma. *Cancer Discov* 9: 1349-1357, 2019.
46. Chester C, Sanmamed MF, Wang J and Melero I: Immunotherapy targeting 4-1BB: Mechanistic rationale, clinical results, and future strategies. *Blood* 131: 49-57, 2018.
47. Gros A, Robbins PF, Yao X, Li YF, Turcotte S, Tran E, Wunderlich JR, Mixon A, Farid S and Dudley ME: PD-1 identifies the patient-specific CD8+ tumor-reactive repertoire infiltrating human tumors. *J Clin Invest* 124: 2246-2259, 2014.
48. Ye Q, Song DG, Poussin M, Yamamoto T, Best A, Li C, Coukos G and Powell DJ Jr: CD137 accurately identifies and enriches for naturally occurring tumor-reactive T cells in tumor. *Clin Cancer Res* 20: 44-55, 2014.
49. Ochoa AC, Zea AH, Hernandez C and Rodriguez PC: Arginase, prostaglandins, and myeloid-derived suppressor cells in renal cell carcinoma. *Clin Cancer Res* 13 (Suppl): 721s-726s, 2007.
50. Yu JW, Bhattacharya S, Yanamandra N, Kilian D, Shi H, Yadavilli S, Katlinskaya Y, Kaczynski H, Conner M, Benson W, *et al*: Tumor-immune profiling of murine syngeneic tumor models as a framework to guide mechanistic studies and predict therapy response in distinct tumor microenvironments. *PLoS One* 13: e0206223, 2018.
51. Segal NH, Logan TF, Hodi FS, McDermott D, Melero I, Hamid O, Schmidt H, Robert C, Chiarion-Sileni V, Ascierto PA, *et al*: Results from an integrated safety analysis of urelumab, an agonist Anti-CD137 monoclonal antibody. *Clin Cancer Res* 23: 1929-1936, 2017.
52. Li Y, Tan S, Zhang C, Chai Y, He M, Zhang CW, Wang Q, Tong Z, Liu K, Lei Y, *et al*: Limited cross-linking of 4-1BB by 4-1BB ligand and the agonist monoclonal antibody utomilumab. *Cell Rep* 25: 909-920.e4, 2018.
53. Chin SM, Kimberlin CR, Roe-Zurz Z, Zhang P, Xu A, Liao-Chan S, Sen D, Nager AR, Oakdale NS, Brown C, *et al*: Structure of the 4-1BB/4-1BBL complex and distinct binding and functional properties of utomilumab and urelumab. *Nat Commun* 9: 4679, 2018.
54. Tolcher AW, Sznol M, Hu-Lieskovan S, Papadopoulos KP, Patnaik A, Rasco DW, Di Gravio D, Huang B, Gambhire D, Chen Y, *et al*: Phase Ib study of utomilumab (PF-05082566), a 4-1BB/CD137 agonist, in combination with pembrolizumab (MK-3475) in patients with advanced solid tumors. *Clin Cancer Res* 23: 5349-5357, 2017.
55. Geuijen C, Tacken P, Wang LC, Klooster R, van Loo PF, Zhou J, Mondal A, Liu YB, Kramer A, Condamine T, *et al*: A human CD137xPD-L1 bispecific antibody promotes anti-tumor immunity via context-dependent T cell costimulation and checkpoint blockade. *Nat Commun* 12: 4445, 2021.
56. Takeda Y, Azuma M, Matsumoto M and Seya T: Tumorcidal efficacy coincides with CD11c up-regulation in antigen-specific CD8(+) T cells during vaccine immunotherapy. *J Exp Clin Cancer Res* 35: 143, 2016.
57. Choi BK, Kim YH, Kang WJ, Lee SK, Kim KH, Shin SM, Yokoyama WM, Kim TY and Kwon BS: Mechanisms involved in synergistic anticancer immunity of anti-4-1BB and anti-CD4 therapy. *Cancer Res* 67: 8891-8899, 2007.
58. Vinay DS and Kwon BS: CD11c+CD8+ T cells: Two-faced adaptive immune regulators. *Cell Immunol* 264: 18-22, 2010.

